Structural Effects in the Reductive Activation of (Indenyl)RhL_2 Complexes: The Reduction of [Rh(η^5-C_9H_7)(η^4-cod)]

Christian Amatore,* Alberto Ceccon, Saverio Santi, and Jean-Noël Verpeaux

Abstract: The reduction of the indenyl complex [Rh(η^5-C_9H_7)(η^4-cod)] has been investigated in the context of structural effects induced by the transfer of one electron. The reduction of this complex occurs in two steps, leading first to the radical anion and then to the highly frangible dianion. Both species eliminate the indenyl anion. In the presence of free cyclooctadiene, the related cleavage leading to the indenyl anion and *bis*-cyclooctadiene rhodium fragments now follows a Michaelis–Menten-type mechanism involving precoordination of one extra COD ligand to the initial radical anion. These results suggest the modification of the hapticity of the indenyl ligand in connection with 17- and 19-electron metal-centered intermediates.

Keywords
electron transfer · indene · kinetics · rhodium

Introduction

The one-electron-transfer activation of coordination complexes of transition metals most generally results in an electronic and structural alteration of the coordination shell in relation to the ability of the metal center(s) or ligands to gain or lose this electron. Structural modifications involving cleavage or formation of chemical bonds can thus be induced in the highly activated species. This may lead to ligand exchange, metal–metal bond formation, or ligand reorganization, all reactions extensively documented in the literature.[1, 2] Among these subsequent processes, changes in the hapticity with redox state is of special interest[3] since the corresponding reversible ligand distortion amounts to a modification of the electronic density at the metal center, which could eventually protect the complex against more drastic reactions (e.g., ligand cleavage). Complexes bearing indenyl (In) ligands are illustrative:[4] for example, reduction of the 18-electron cation $[(\eta^5\text{-In})_2V(CO)_2]^+$ gives the $[(\eta^5\text{-In})(\eta^3\text{-In})V(CO)_2]$ radical after slippage of one five-membered ring,[5] whereas the same treatment of the corresponding cyclopentadienyl complex $[Cp_2V(CO)_2]$ leads to the cleavage of a molecule of CO.

This possibility of accommodating various electronic environments provides chemical flexibility associated with enhanced reactivity (the indenyl effect),[6] which justifies quantitative investigation of this indenyl slippage process (Scheme 1).

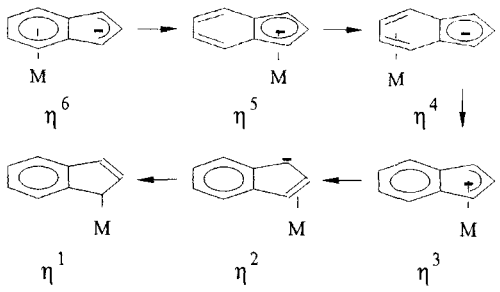

Scheme 1. The indenyl slippage process.

[(In)RhL_2] (In = indenyl) complexes have proven to be very efficient catalysts for the hydroacylation of olefins, cyclotrimerization of alkynes or even hydrocarbon CH bond activation.[7] The "indenyl effect" is quite strong in this series; it was shown that a ligand exchange reaction became faster by a factor of 10^8 when the cyclopentadienyl ligand in [CpRhL_2] was replaced by the indenyl ligand. Since the catalytic efficiency is also heavily dependent on the ability to accommodate new ligands in and out of the coordination shell, it was decided to investigate the effect of electron-transfer activation on the structural properties of the complex [(In)Rh(cod)], where cod is cyclooctadiene, both in the presence and absence of extra ligand. Kinetic data allowed the range of stability and reactivity of the monoanion $[(In)Rh(cod)]^-$ to be established (in the presence and absence of free COD), and finally to propose a mechanism for the stepwise decoordination of indenyl involving a precoordination of a second COD ligand (see Scheme 3).

[*] C. Amatore, J.-N. Verpeaux
Département de Chimie de l'Ecole Normale Supérieure, URA CNRS 1679
24 rue Lhomond, F-75231 Paris cedex 05 (France)
Fax: Int. code +(1)4432-3325
e-mail: amatore@chimene.ens.fr
A. Ceccon, S. Santi
Università degli Studi di Padova, Dipartimento di Chimica Fisica
Via Loredan 2, I-35131 Padova (Italy)

Results and Discussion

Delineation of reactivity induced by electron transfer

Reduction of [(In)Rh(cod)] alone: As shown in Figure 1, the cyclic voltammogram at 0.5 Vs^{-1} of a 3 mM solution of the title compound in THF/0.3 M $nBu_4N \cdot BF_4$ exhibited two reduction

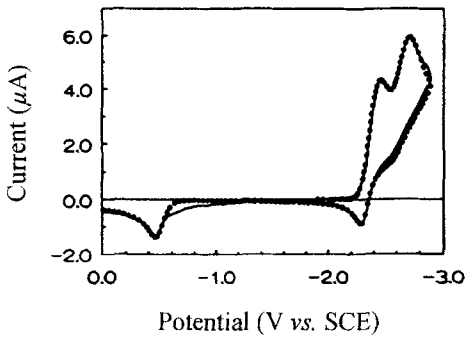

Figure 1. Experimental (solid line) and simulated (circles) voltammetric reduction of [(In)Rh(cod)], 3 mM, in THF/0.3 M $nBu_4 \cdot BF_4$ at a gold disk electrode (0.5 mm diameter); $v = 0.5\ Vs^{-1}$, 20 °C. Thermodynamic and kinetic parameters used in the simulated voltammogram: $E_1^0 = -2.35$ V vs. SCE, $k_1^0 = 5 \times 10^{-3}\ cm\,s^{-1}$, $\alpha_1 = 0.35$, $E_2^0 = -2.65$ V vs. SCE, $k_2^0 = 5 \times 10^{-3}\ cm\,s^{-1}$, $\alpha_2 = 0.35$, $k_f = 0.6\ s^{-1}$, $k_b = 5\ M^{-1}s^{-1}$ and $k \geq 2 \times 10^3\ s^{-1}$ (see text and experimental section) [14].

waves at rather negative potentials. The first wave was chemically partially reversible although electrochemically irreversible ($\alpha = 0.35$, $\Delta E^p = E_{ox}^p - E_{red}^p = 140$ mV at $0.5\ Vs^{-1}$) whereas chemically the second wave was totally irreversible. The peak current function of the first wave, that is, $i^p v^{-1/2}$, was not constant with the scan rate (Figure 2), thus establishing that the first reduction wave involved a subsequent reaction coupled with further electron transfer.[8]

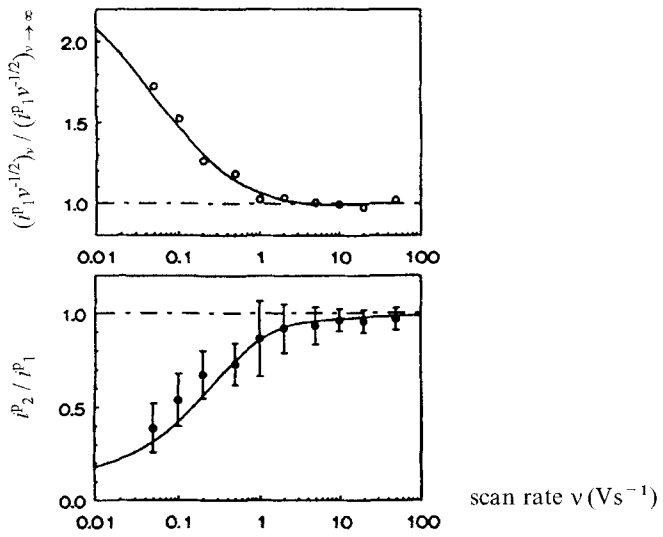

Figure 2. Variations of the current function ($i_1^p v^{-1/2}$) of the first reduction wave (top) and of the ratio (i_2^p/i_1^p) of the peak current of the second and first reduction wave (bottom) of [(In)Rh(cod)], 15 mM in THF/0.3 M $nBu_4 \cdot BF_4$ at a gold disk electrode (0.5 mm, 0.125 mm or 25 μm diameter according to the scan rate), 20 °C. Symbols: experimental data; solid lines: theoretical variations based on simulations using the set of thermodynamic and kinetic parameters given in Figure 1. Note that the current function (top) is normalized to its value at infinite scan rate (here $v > 100\ Vs^{-1}$) where the wave obeys a chemically reversible but slow charge transfer kinetic regime [8]; because of this choice the normalized current function reaches values larger than two at low scan rates, although this corresponds to a two-electron limit.

Determination of the absolute electron stoichiometry[9] at sufficiently high scan rate ($v \geq 2\ Vs^{-1}$) showed that within this timescale the first wave corresponds to a one-electron process ($n_{app} = 1.2 \pm 0.2$). This process was associated with the observation of a chemically fully reversible wave, provided that the scan was inverted between the two reduction waves. Both facts indicate that the anion radical $[(In)Rh(cod)]^-$ is the reduction product for the first wave [Eq. (1)], provided that the timescale is short enough, that is, $v \geq 2\ Vs^{-1}$.

At lower scan rates, for example $0.5\ Vs^{-1}$ (Figure 1), this intermediate is not fully stable, as indicated by the growth of the current function of the first peak ($n_{app} > 1$) and by the partial loss of chemical reversibility of the wave. The second wave can then be assigned a priori either to the further reduction of the anion radical, or to the reduction of one of the products formed by evolution of the anion radical. The fact that the second wave corresponds to the further reduction of the anion radical to the dianion $[(In)Rh(cod)]^{2-}$ [Eq. (3)] was established by the observation that at large scan rates ($v \geq 2\ Vs^{-1}$) the two reduction waves had approximately the same size (viz., corresponded to one electron each). Thus, when the decomposition of $[(In)Rh(cod)]^-$ was suppressed, the amount of species reduced at the second wave was quantitative (Figure 2). Despite its one-electron stoichiometry, the second wave remained chemically irreversible over the complete range of scan rates investigated ($v \leq 100\ Vs^{-1}$), which showed that the dianion was considerably less stable [$t_{\frac{1}{2}} < 0.2$ ms, Eq. (4)] than the anion radical. Chronoamperometric experiments in which $i(\theta)$, the current measured at the end of a potential step of duration $\theta = 0.2$ s, was plotted as a function of the step potential confirmed the existence of a monoelectronic reduction when $E_{step} > -2.55$ V and of a bielectronic overall reduction at more negative values.

$$[(In)Rh(cod)] + e^- \rightleftharpoons [(In)Rh(cod)]^- \quad (E_1^0 = -2.35\ V\ vs\ SCE) \quad (1)$$

$$[(In)Rh(cod)]^- \dashrightarrow \text{etc.} \quad (v < 2\ Vs^{-1}) \quad (2)$$

$$[(In)Rh(cod)]^- + e^- \longrightarrow [(In)Rh(cod)]^{2-} \quad (E_2^p = -2.72\ V\ at\ 0.5\ Vs^{-1}) \quad (3)$$

$$[(In)Rh(cod)]^{2-} \longrightarrow \text{etc.} \quad (\text{fast}, t_{\frac{1}{2}} < 0.2\ ms) \quad (4)$$

The gradual loss of reversibility of the first reduction wave on increasing the timescale (decreasing the scan rate) associated with a concomitant rise of the current function (Figure 2) suggested that Equation (2) corresponds in fact to the setting up of an ECE/disproportionation process[10] in which the anion radical formed in the first wave generated a product that was quantitatively reduced at this potential.

Figure 1 shows that an oxidation wave at −0.43 V is present on the reverse potential scan provided that the potential scan is inverted after the first reduction peak. This wave is much more intense when the potential is reversed after the second reduction wave. It could be assigned to the oxidation of the indenyl anion by comparison with an authentic sample generated by in situ deprotonation of indene. This indicates that the indenyl anion, In^-, is a common reaction product of each redox process.

Reduction of [(In)Rh(cod)] in the presence of free COD: The reduction of [(In)Rh(cod)] in the presence of one equivalent of COD was then investigated. Figure 3a shows the voltam-

0947-6539/97/0302-0280 $ 15.00+.25/0 Chem. Eur. J. 1997, 3, No. 2

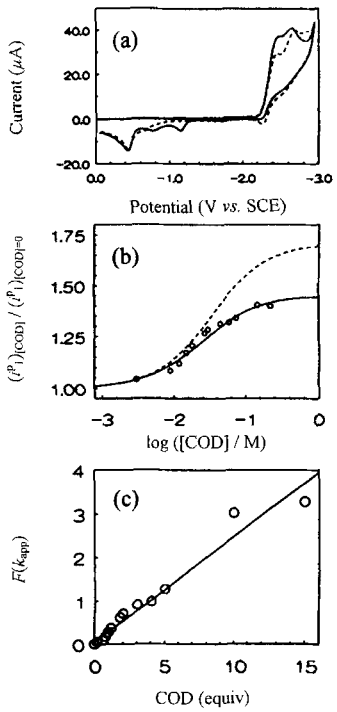

Figure 3. Voltammetric reduction of [(In)Rh(cod)], 15 mM, in THF/0.3 M $nBu_4 \cdot BF_4$ at a gold disk electrode (0.5 mm diameter), in the presence of added COD; $v = 0.5\ Vs^{-1}$, 20 °C. a) Voltammograms in the absence (dashed line) or in the presence (solid line) of one equivalent of COD. b) Experimental (open circles) or theoretical (solid line) variations of the peak current of the first reduction wave normalized to its value in the absence of COD. The theoretical curve was obtained by simulation based on the set of thermodynamic and kinetic parameters given in Figure 1 and $k^* = 10.5\ s^{-1}$, $\rho = k_3/(1 + k_{-3}/k^*) = 1.5\ M^{-1}s^{-1}$ (see text). The dashed line is the theoretical prediction for a classical S_N2 mechanism (as in Scheme 2). Note that although the limit of the dashed line at infinite COD concentration corresponds to a two-electron process, it appears smaller in the Figure because of the normalization used, since the peak current in the absence of added COD already corresponds to 1.15 electron per mole. c) Plot of the same experimental data as in (b) in the form of Equation (17); the regression line (correlation coefficient 0.985) corresponds to $k^* = 10.5\ s^{-1}$ and $\rho = k_3/(1 + k_{-3}/k^*) = 1.5\ M^{-1}s^{-1}$, and is identical to the solid working curve in (b).

mograms obtained before (dashed line) and after (solid line) the addition of the free ligand. Comparison of such voltammograms indicates that, within the same timescale (i.e., at constant potential scan rate), addition of COD results in 1) an increase of the peak current and a loss of reversibility of the first reduction wave, 2) a decrease of the peak current of the second one associated with a marked positive shift of its peak potential (50 mV for one equivalent of COD added at $0.5\ Vs^{-1}$), and 3) the observation on reverse potential scan of a set of two new oxidation waves of nearly equal intensity (at $E^p - 1.15$ and -0.78 V versus SCE for $v = 0.5\ Vs^{-1}$) in addition to the oxidation wave of the indenyl anion.

An independent study of the voltammetric reduction of an authentic sample of $[Rh(cod)_2]^+$ in the same medium led to the observation of two consecutive one-electron reduction waves corresponding to the cation/radical and radical/anion redox couples, in agreement with previous observations, albeit in different solvents.[11] The position of the waves allowed assignment of the new set of oxidation waves in Figure 3a to the successive monoelectronic oxidation of $[Rh(cod)_2]^-$ and $[Rh(cod)_2]$, respectively.

Kinetics and mechanism

Mechanism in the absence of free ligand: In the absence of free COD ligand, the electrochemical reduction of [(In)Rh(cod)] led to the monoanion and then, at a more negative potential, to the dianion. The dianion is very unstable, its lifetime being less than 0.2 ms, and undergoes a fast cleavage of the indenyl anion, oxidation of which was observed at -0.43 V. Thus, a reasonable description of the process at the second wave can be given according to Equations (3), (5), and (6).

$$[(In)Rh(cod)]^{2-} \longrightarrow In^- + [Rh(cod)]^- \quad (k > 2 \times 10^3\ s^{-1}) \quad (5)$$

$$[Rh(cod)]^- \longrightarrow \text{degradation products} \quad (6)$$

$[Rh(cod)]^-$ represents an unstable, unsaturated anionic rhodium fragment. No direct information concerning the nature or the fate of this rhodium center could be obtained in this study,[12] since no wave that could have been ascribed to this species was visible on the cathodic or anodic voltammetric scans. Such an unsaturated rhodium anion is not expected to be stable, since it is formally a 14-electron complex, which may explain why no electroactive fragment could be detected in the absence of extra ligand. Note that the observation of rhodium bis(cyclooctadiene) redox couples in the presence of added cyclooctadiene also supports the formation of a $[Rh(cod)]^-$ fragment in the absence of COD.

The anion radical is far more stable; nevertheless, it afforded, through a route involving uptake of an additional electron, the same indenyl anion formed by cleavage of the dianion [Eq. (5)]. Two possible routes could be proposed to account for this behavior. One consists of a slow endergonic disproportionation [Eq. (7)], leading to the dianion and thus being continuously displaced by its fast cleavage [Eq. (5)]. This route could be ruled

$$2[(In)Rh(cod)]^- \longrightarrow [(In)Rh(cod)] + [(In)Rh(cod)]^{2-} \quad (\Delta G^0 = F(E_1^0 - E_2^0) > 0) \quad (7)$$

out based on the fact that the chemical irreversibility of the first wave was independent of the concentration of the substrate.[13] A second route consists of an ECE/DISP sequence,[10] in which the anion radical underwent a slow cleavage, leading to the indenyl anion and to a reducible rhodium-centered fragment. According to simple stoichiometry, this rhodium species must be [Rh(cod)], reduction of which at the electrode surface (or homogeneously) should afford the same $[Rh(cod)]^-$ fragment as that formed on decomposition of the dianion [Eq. (5)]. All the experimental observations converge, therefore, on the mechanism at the first reduction wave being described by Equations (8)–(10).

$$[(In)Rh(cod)] + e^- \rightleftharpoons [(In)Rh(cod)]^- \quad (E_1^0 = -2.35\ V \text{ vs SCE}) \quad (8)$$

$$[(In)Rh(cod)]^- \longrightarrow [Rh(cod)] + In^- \quad (9)$$

$$[Rh(cod)] + e^- \longrightarrow [Rh(cod)]^- \quad (E^p > E_1^0) \quad (10)$$

Quantitative assessment of the two mechanisms described above could be performed only based on simulation procedures because of the intrinsic slowness of the two electron transfers [Eqs. (3) and (8)]. The rate of electron transfer for Equation (8) ($k_1^0 = 5 \times 10^{-3}\ cm\,s^{-1}$) was adjusted based on the peak-to-peak separation[8] of the first wave at high scan rates ($v > 5\ Vs^{-1}$), where the wave was chemically reversible.[14] An arbitrary rate constant for the cleavage of the dianion [Eq. (5)] was chosen to be sufficiently large for the simulations to result independent of this parameter. Therefore the simulations of a series of voltammograms at moderate scan rates ($v < 5\ Vs^{-1}$) required only determination of the rate constant for the cleavage of the anion radical [Eq. (9)].

First, this parameter was adjusted ($k_f = 0.6\ s^{-1}$) to reproduce the experimental dependence of the peak current of the first wave as a function of the scan rate (compare Figure 2). However, and despite the good agreement between simulations and

experimental results for the peak current, we found that this rate constant led to a degree of reversibility of the first wave that was slightly smaller than the experimental value, especially when the second wave was scanned before the potential scan inversion. This result indicates that products formed at the second wave could affect the overall stability of the anion radical. The most simple explanation to account for this phenomenon is that the cleavage of the anion radical is slightly reversible. The effect of such a slight reversibility could be negligible at the level of the first peak current, where the flux production of the stable indenyl anion is small. Conversely, because scanning the second wave resulted in the build-up of a quantitative concentration of indenyl anion in the diffusion layer, a bimolecular reverse reaction could lead to partial reversal of the cleavage reaction, leading then to an apparent increase in the reversibility of the first wave. The validity of this hypothesis was checked by means of simulations based on the above value of k_f, by adjusting the rate constant k_b of the reverse reaction so that the experimental degree of reversibility could be correctly reproduced in the simulations ($k_b = 5\,M^{-1}s^{-1}$) [Eq. (11)].[15]

$$[(In)Rh(cod)]^- \underset{k_b}{\overset{k_f}{\rightleftharpoons}} [Rh(cod)] + In^- \qquad (11)$$

The rate constants k_f and k_b of the forward and reverse reactions, respectively, were thus determined and the mechanistic sequence [Eqs. (8), (11), and (10)] demonstrated. Note that it can be seen from the small value of k_b (which leads to a pseudo-first-order rate in the range of $0.01\ s^{-1}$ for a 2 mM substrate concentration) that the coupling between indenyl anion and the Rh(cod) fragment is not a favorable process unless the concentration of indenyl anion is high and the equilibrium displaced toward its left-hand-side by the reoxidation of the $[(In)Rh(cod)]^-$ anion radical. This explains why the current function of the first reduction wave depended almost exclusively on the forward process (i.e., on k_f)[15] while the reversibility of the wave was also a function of the reverse reaction [Eq. (11)], that is, of k_b and of the concentration of the indenyl anion, that is, the point of inversion of the potential scan.

Mechanism in the presence of free COD: The presence of free COD ligand provided further support for Equations (5) and (11), since this allowed the rhodium fragments to be stabilized by COD coordination, thus permitting their identification based on the observation of the characteristic system of paired one-electron waves due to the sequential oxidation of the anion $[Rh(cod)]^{2-}$ and of the radical $[Rh(cod)_2]$[11] Thus, the formation of indenyl anion on the one hand, and rhodium bis(cyclooctadiene) anion on the other, both detected by their oxidation wave on the reverse scan, suggest that the same overall reactivity was preserved in the absence of COD.

The increase of the first reduction wave at the expense of the second, as well as the loss of reversibility when COD is added to the solution, indicates decreased stability of $[(In)Rh(cod)]^-$ in the presence of COD. One could argue that this effect is only indirect and reflects suppression of the reverse reaction [Eq. (11)] because of a fast stabilization of the rhodium fragment by COD coordination after the cleavage. This first interpretation was rejected, however, because we saw above that the reverse reaction does not significantly influence the current function of the first wave. Since this is mainly a function of the forward step (i.e., of k_f, which would not be modified in this process) we are forced to conclude that COD reacts directly with the anion radical (in an associative mechanism), in competition with Equation (11), that is, with the former spontaneous decomposition of this species.

The mechanistic sequence shown in Scheme 2 is kinetically equivalent to that in Equations (8)–(10), with an apparent rate

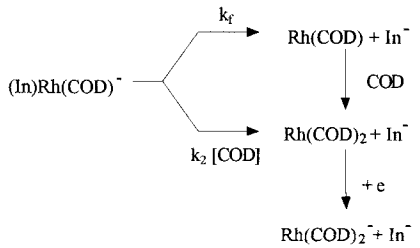

Scheme 2. Mechanistic sequence of the overall decomposition of the anion radical $[(In)Rh(cod)]^-$.

constant $k_{app} = k_f + k_2[COD]$ for the overall decomposition of the anion radical $[(In)Rh(cod)]^-$.[16] Accordingly, this apparent rate constant should be made as large as desired just by increasing the concentration of COD. That means that for a given scan rate, it should be possible to make k_{app} sufficiently large to reach the two-electron limit of the ECE process simply by increasing the excess of COD. Conversely, at a given COD concentration, the same two-electron limit should be achieved by decreasing the potential scan rate v (compare, e.g., the analogous effect in Figure 2), since the actual parameter that governs the current function of the first peak is then $k_{app}/v = (k_f + k_2[COD])/v$.[10] Experimentally, we did not observe such symmetric roles for [COD] and scan rate. Indeed, if a two-electron limit could be reached on decreasing the scan rate, the limit reached by increasing the COD concentration at a given scan rate was significantly lower (Figure 3b) and, furthermore, depended on the scan rate, being closer to the two-electron limit the smaller the scan rate. This asymmetry is sufficient to rule out the occurrence of the mechanism in Scheme 2, at least within its present formulation.

The existence of a limit less than the expected two-electron limit on increasing the COD concentration implied a leveling of its effect. The simplest way to account for such a saturation within the framework of Scheme 2 was to consider a Michaelis–Menten-like mechanism, in which the COD-assisted cleavage of $[(In)Rh(cod)]^-$ occurs by a two-step mechanism involving reversible addition of COD to the anion radical followed by a fast, irreversible cleavage of the adduct [Eqs. (12) and (13)] that is

$$[(In)Rh(cod)]^- + cod \underset{k_{-3}}{\overset{k_3}{\rightleftharpoons}} [(In)Rh(cod)_2]^- \qquad (12)$$

$$[(In)Rh(cod)_2]^- \xrightarrow{k^*,\,fast} [Rh(cod)_2] + In^- \qquad (13)$$

COD-independent. At sufficiently low COD concentration, the equilibrium according to Equation (12) is expected to lie mostly to the left-hand side. Thus, the apparent rate law for the chemical decomposition of the anion radical can be expressed simply as Equation (14), showing that the whole sequence then behaves

0947-6539/97/0302-0282 $ 15.00+.25/0 Chem. Eur. J. 1997, 3, No. 2

as explained above for Scheme 2, with k_2 now being equal to $k^*k_3/(k^* + k_{-3})$. This scheme predicts an increase in the current

$$d[(In)Rh(cod)^-]/dt \approx -\left\{\frac{k^*k_3}{k^* + k_{-3}}[COD] + k_f\right\}[(In)Rh(cod)^-] \quad (14)$$

function of the first wave with an increase in the COD concentration or a decrease in the scan rate. Conversely, at sufficiently high COD concentration, the equilibrium in Equation (12) is expected to be shifted completely toward the right-hand side. The kinetics of the sequence given by Equations (12) and (13) is then controlled only by the rate of cleavage of the adduct, that is, by k^*. The current function, therefore, becomes independent of the COD concentration, but still increases with a decrease in the scan rate.

Therefore, the sequence in Equations (12) and (13) qualitatively explains the experimental behavior described above. In a general case, that is, when [COD] is not an extreme value, the system still behaves as an ECE sequence [i.e., as given in Eqs. (8)–(10)] with an apparent rate constant k_{app} for the decay of the anion radical given by Equations (15) and (16).

$$d[(In)Rh(cod)^-]/dt \approx -k_{app}[(In)Rh(cod)^-] \quad (15)$$

$$k_{app} = k^*\left[1 + \frac{k_f - k^*}{k^* + k_3[cod]/(1 + k_{-3}/k^*)}\right] \quad (16)$$

When [COD] is sufficiently small for $[COD] \ll (k^* + k_{-3})/k_3$, one obtains $k_{app} \approx k_f + k_3k^*[COD]/(k^* + k_{-3})$, which then leads to a rate expression identical to the above limiting Equation (14). Conversely, when [COD] is sufficiently large for the condition $[COD] \gg (k^* + k_{-3})/k_3$ to be true, Equation (16) can be simplified into $k_{app} \approx k^*$, which shows that the rate of cleavage of the anion radical becomes independent of the COD concentration. One interesting aspect of this latter limiting case is that it allows the independent determination of k^* (i.e., $k^* = 10.5\ s^{-1}$) based on the scan rate dependence of the current function measured at high COD concentration, that is, in the range of concentration where the current function is dependent on the scan rate but is independent of [cod] (compare Figure 3b). Independent knowledge of k^* and k_f allows Equation (16) to be rewritten as Equation (17). This formulation

$$F(k_{app}) = (k_{app} - k_f)/(k^* - k_{app}) = [k_3/(k^* + k_{-3})][COD] = (\rho/k^*)[COD] \quad (17)$$

shows that the function $F(k_{app})$, which can be evaluated from the experimental k_{app} values determined by simulating at each scan rate and COD concentration a simple irreversible ECE sequence[10] (vide supra for the determination of k_f), must depend linearly on [COD]. This is actually what is observed in Figure 3c,[17] thereby supporting the above mechanism [Eqs. (12) and (13)]. Furthermore, from the slope of the regression line and from independent knowledge of k^*, the rate parameter ρ ($\rho = k_3/(1 + k_{-3}/k^*) = 1.5\ M^{-1}s^{-1}$) can be determined. Note, however, that the individual rate constants k_3 and k_{-3} cannot be determined because the current function is independent of their actual values but depends only on k_f, k^*, and ρ [compare with Eq. (16)]. Based on the knowledge of these three rate parameters, the theoretical variations of the current function of the first wave can be simulated as a function of the COD concentration at any scan rate based on the complete mechanism [namely, Eqs. (8), (12), (13) followed by the exergonic reduction of $[Rh(cod)_2]$] and compared with the experimental dependence. It is seen in Figure 3b that the agreement between experimental determination and prediction (solid line) is excellent, providing additional support for the validity of the mechanism represented by Equations (12) and (13).

Structural aspects: Electrochemical methods are quite efficient for picturing intermediates and providing kinetic data necessary to build reactivity schemes. Unfortunately, they are less well-suited to solving the structure of these intermediates. This is particularly true in the case of 17- versus 19-electron complexes, as recently stressed.[3] The following section presents a reasonable structural interpretation of the reactivity scheme established above.

There is no doubt that the thermodynamically favored structure of [(In)Rh(cod)] corresponds to an 18-electron compound with an η^5 indenyl ligand. On the other hand, the dianion formed after the second electron transfer must correspond to a η^3 indenyl hapticity to avoid a 20-electron metal configuration.[19] The required ring slippage is known to be easy in indenyl complexes.[6] Regarding the intermediate anion radical, things are less obvious and two possibilities (17-electron complex with η^3 indenyl ligand or 19-electron complex with η^5 hapticity) must be considered.[3, 4] In the absence of spectroscopic or structural data, nothing definitive can be formulated. However, several facts have been established in this work: 1) the peak-to-peak separation of the reversible first reduction wave is large and its transfer coefficient small ($\Delta E^p = E^p_{ox} - E^p_{red} = 140$ mV, $\alpha = 0.35$, at $v = 0.5\ Vs^{-1}$) suggesting that an important structural rearrangement is associated with the electron transfer. 2) The second reduction takes place only about 300 mV after the first. This gap is quite small compared with the usual separation between the reduction waves of a neutral species and its anion radical in THF due to coulombic repulsion. For example, for conjugated organic molecules such as azobenzene this gap is in the 600 mV range under the same conditions. A comparison with other organometallic compounds is certainly more relevant: the two reduction waves of the 16-electron $[Rh(cod)_2]^+$ are also separated by ca. 600 mV in chlorinated solvents or acetone[11] and approximately 500 mV in THF. Data concerning 18-electron compounds cannot be used so easily, because they necessarily raise the same problem of the 17- versus 19-electron structure of the first reduced species, as illustrated by the example of indenyl tris carbonyl manganese.[18] The small gap observed in our case indicates that the effect of the coulombic repulsion (ca. 50–55 kJ mol^{-1} based on a peak separation of 500–600 mV) is counteracted by a decrease of the standard reduction potential of the anion radical vis-à-vis its would-be 19 electron structure. Based on the experimental peak separation of ca. 300 mV, the reduction potential is shifted by ca. 20–30 kJ mol^{-1}. This observation is better accounted for when assuming that a 17- rather than a 19-electron anion is being reduced at the second wave.[3] 3) The radical anion at hand has been shown to coordinate an extra COD ligand readily [Eq. (12)], which is also indicative of a hypovalent complex. All these three arguments point to the reduction of a 17-electron anion radical, that is, with $\eta 3$ hapticity, at the second wave.[19] This may correspond either to a true 17-electron structure or to

a fast CE sequence[8] involving a rapid equilibrium between 19- and 17-electron forms that would provide the same kinetic data when quenching the 17-electron intermediate by reduction at the second wave or by COD coordination. In other words, the results obtained here support a ring slippage towards the allyl-like coordination associated with the first electron transfer or a very labile structure for the radical anion due to a low barrier between the 17- and 19-electron isomers.[20] It is impossible to distinguish firmly between the two possibilities on the basis of the present results.

The fact that this radical anion $[(In)Rh(cod)]^-$ adds a free COD ligand [Eq. (12)] before cleavage of the rhodium-indenyl bond [Eq. (13)] has been established on kinetic grounds. The small but significant (50 mV) positive shift of the second reduction peak observed on addition of free COD (see Figure 3) provides additional support[21] for such an associative mechanism with formation of an intermediate adduct [Eqs. (12) and (13)] by opposition to the simple associative mechanism initially considered in Scheme 2. Indeed, the latter case would imply that the second wave still corresponds to the reduction of the same species $[(In)Rh(cod)]^-$ as in the absence of COD, whereas in the Michaelis–Menten-like process the second wave must be assigned to the reduction of the adduct, the stoichiometry of which is $[(In)Rh(cod)_2]^-$.

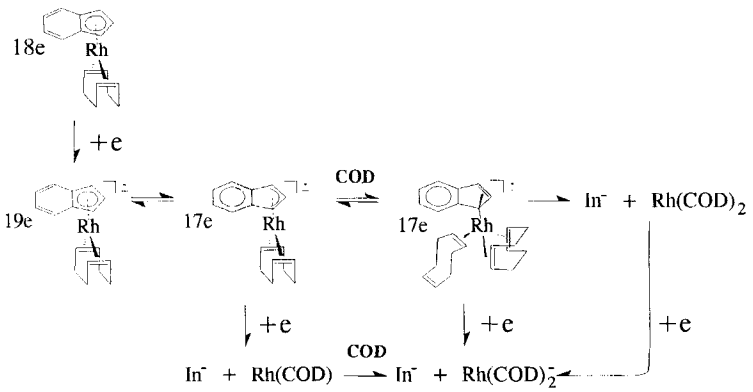

Scheme 3. Topological processes triggered by the electron transfer activation of [(In)Rh(cod)] in the presence of free COD.

It is remarkable that this adduct, which bears the same charge as and more ligands than the parent mono-COD anion radical, is reduced at a potential very close to and even slightly more positive than the reduction potential of the parent $[(In)Rh(cod)]^-$. This result suggests that the electronic density around the metal center is quite similar in both cases. Consequently, if $[(In)Rh(cod)]^-$ is to be depicted as $[(\eta^3\text{-In})Rh(\eta^4\text{-cod})]^-$, the bis(COD) radical anion can be regarded either as $[(\eta^3\text{-In})Rh(\eta^2\text{-cod})_2]^-$ or as $[(\eta^1\text{-In})Rh(\eta^4\text{-cod})(\eta^2\text{-cod})]^-$. On the other hand, the adduct undergoes a fast cleavage of the indenyl anion, at least compared with the parent mono(COD) anion radical ($k^* = 10.5\ s^{-1}$ vs. $k_f = 0.6\ s^{-1}$). This would rather favor a weaker association of the indenyl ligand and consequently η^1-hapticity for the indenyl ligand. The overall dance of the rhodium center on the indenyl ring ends here with the cleavage of the indenyl anion. Scheme 3 summarizes the topological processes triggered by the electron transfer activation of [(In)Rh(cod)] in the presence of free ligand.

Experimental Section

Chemicals and Instrumentation: THF was purified by distillation from sodium benzophenone under argon and thoroughly degassed. Fluorenone (Aldrich) was used without further purification; cyclooctadiene (Aldrich) was redistilled prior to use. The starting complexes [(indenyl)Rh(cod)] [22] and $[Rh(cod)_2]BF_4$ [23] were synthetized according to published procedures. (Indenyl)K was prepared by deprotonation of freshly distilled indene (0.1 M solution in THF) by 10 equivalents of potassium hydride under argon.

All the electrochemical experiments were run under argon. nBu$_4$N·BF$_4$ was used as the supporting electrolyte; it was obtained from nBu$_4$N·HSO$_4$ and NaBF$_4$ and recrystallized from ethyl acetate/hexane. Cyclic voltammetry experiments were performed in an air-tight three-electrode cell connected to a vacuum line. The reference electrode was SCE (Tacussel ECS C10) separated from the solution by a bridge compartment filled with the same solvent/supporting electrolyte solution as that used in the cell. The counter electrode was a platinum spiral with ca. 1 cm^2 apparent surface area. The working electrodes were disks obtained from cross-sections of gold wires of various diameters (0.5 or 0.125 mm and 25 μm) sealed in glass. Between each CV scan the working electrodes were polished on alumina according to standard procedures and sonicated before use. A EG&G PAR-175 signal generator was used. The potentiostat was home-made [24], with a positive feedback loop for ohmic drop compensation. The currents and potentials were recorded on Nicolet 310 or Lecroy 9310L oscilloscopes.

Determination of the absolute electron stoichiometry [9]: The steady-state reduction currents at a 12.5 μm radius gold disc microelectrode (potential scan rate 50 mVs^{-1}) and the chronoamperometric diffusional currents at a 0.5 mm diameter electrode for a step duration of 0.2 s were measured for a 3 mM solution of [(In)Rh(cod)] and fluorenone ($D = 1.017 \times 10^{-5}\ cm^2 s^{-1}$) under identical conditions (THF, 0.28 M nBu$_4$N·BF$_4$). These data allowed the determination of the absolute consumption of electrons at the first reduction wave of [(In)Rh(cod)] and the diffusion coefficient of this rhodium complex in this medium. For a characteristic time of 0.2 s the results were $n_{app} = 1.2 \pm 0.2$ and $D = (1.34 \pm 0.18) \times 10^{-5}\ cm^2 s^{-1}$.

Simulations: Digital simulations of the voltammograms corresponding to the proposed mechanisms were performed with the program elaborated by D. Gosser [25], from the set of values indicated in the captions of Figures 1 and 3. The thermodynamic and kinetic parameters featuring the first reduction wave were determined from the experimental voltammograms following the procedures indicated in the text. This led to a set of thermodynamic (E_1^0), heterogeneous kinetic (α_1, k_1^0), and homogeneous kinetic (k_f, k_b, k^*, and ρ) parameters that is really characteristic of the electron transfer and subsequent kinetics involved in the first reduction wave. The situation is different for the second wave. Formally, its simulation requires independent knowledge of the thermodynamic (E_2^0) and kinetic (α_2, k_2^0) parameters of the electron transfer, as well as the rate constant (k) of the cleavage of the dianion [eq. (5)]. However, since this wave is controlled by the kinetics of electron transfer, its shape and position are independent of the value of k, provided that this value is large enough to lead to a chemically irreversible wave at each scan rate considered [8]. Thus, a value for k of $2 \times 10^3\ s^{-1}$ was used, although this value represents only a minimum value of the true rate constant in equation (5). $\alpha_2 = 0.35$, used in the simulations, was determined from the experimental half-width of the second reduction peak [8]. Owing to its charge transfer control, the position of the second reduction peak depends only on the value of the global parameter $E_2^0 + (RT/\alpha_2 F)\ln k_2^0$ [8], and not on the individual values of E_2^0 and k_2^0. Therefore, choosing arbitrarily $k_2^0 = k_1^0$ in the simulations [14] implied the use of a value for E_2^0 such as $E_2^0 - E_1^0 = E_2^p - E_1^p$. Using the experimental value for $E_2^p - E_1^p$ of -0.30 V at 0.5 Vs^{-1}, and $E_1^0 = 2.35$ V vs. SCE thus imposed an arbitrary value of $E_2^0 = -2.65$ V vs. SCE in the simulations. However, it should be emphasized that the set of E_2^0, k_2^0, and k values used in the simulations should not be considered individually but just as a coherent set allowing the simulation of the shape and position of the second wave.

0947-6539/97/0302-0284 $ 15.00+.25/0 Chem. Eur. J. 1997, 3, No. 2

Acknowledgements: This work was supported in part by the CNRS and ENS for the French team and by the University of Padova and CNR for the Italian one. A bilateral international collaborative research grant cofunded by CNRS (France) and CNR (Italy) is also gratefully acknowledged.

Received: June 7, 1996 [F387]

[1] a) N. G. Connelly, W. E. Geiger, *Adv. Organomet. Chem., Vol. 23* (Eds.: F. G. A. Stone, R. West), Academic Press, Orlando, **1984**, pp. 1–93; b) *Organometallic Radical Processes* (Ed.: W. C. Trogler), J. Organomet. Chem. Library, Elsevier, Amsterdam, **1990**.

[2] a) J. K. Kochi, *Organometallic Mechanisms and Catalysis*, Academic Press, New York, **1978**; b) D. Astruc, *Chem. Rev.* **1988**, *88*, 1188; c) D. R. Tyler, *Acc. Chem. Res.* **1991**, *24*, 325.

[3] W. E. Geiger, *Acc. Chem. Res.* **1995**, *28*, 351 and references therein.

[4] K. A. Pevear, M. M. Banaszak Holl, G. B. Carpenter, A. L. Rieger, P. H. Rieger, D. A. Sweigart, *Organometallics*, **1995**, *14*, 512.

[5] a) G. A. Miller, M. J. Therien, W. C. Trogler, *J. Organomet. Chem.* **1990**, *383*, 271; b) R. M. Kowaleski, A. L. Rheingold, W. C. Trogler, F. Basolo, *J. Am. Chem. Soc.* **1986**, *108*, 2460.

[6] a) M. E. Rerek, L. N. Ji, F. J. Basolo, *J. Chem. Soc. Chem. Commun.* **1983**, 1208; b) J. M. O'Connor, C. P. Casey, *Chem. Rev.* **1987**, *87*, 307; c) Y. M. Wuu, C. Zou, M. S. Wrighton, *J. Am. Chem. Soc.* **1987**, *109*, 5861; d) A. K. Kakkar, N. J. Tayor, T. B. Marder, J. K. Shen, N. Hallinan, F. Basolo, *Inorg. Chim. Acta* **1992**, *198*, 219; e) O. V. Gusev, L. I. Denisovich, M. G. Peterleitner, A. Rubezhov, N. A. Ustynyuk, P. M. Maitlis, *J. Organomet. Chem.* **1993**, *452*, 222; f) A. Ceccon, C. J. Elsevier, J. M. Ernsting, A. Gambaro, A. S. Santi, A. Venzo, *Inorg. Chim. Acta* **1993**, *204*, 15.

[7] a) A. Borrini, P. Diversi, G. Ingrosso, A. Lucherini, G. Serra, *J. Mol. Catal.* **1985**, *30*, 181; b) T. B. Marder, D. C. Roe, D. Milstein, *Organometallics* **1988**, *7*, 1451. c) A. Ceccon, A. Gambaro, S. Santi, A. Venzo, *J. Mol. Catal.* **1991**, *69*, L1. d) T. M. Frankcom, J. C. Green, A. Nagy, A. K. Kakkar, T. B. Marder, *Organometallics* **1993**, *12*, 3688.

[8] A. J. Bard, L. F. Faulkner, *Electrochemical Methods*, Wiley, New York, **1980**.

[9] C. Amatore, M. Azzabi, P. Calas, A. Jutand, C. Lefrou, Y. Rollin, *J. Electroanal. Chem.* **1990**, *288*, 45.

[10] C. Amatore, J. M. Savéant, *J. Electroanal. Chem.* **1978**, *86*, 227; *ibid.* **1979**, *102*, 21.

[11] J. Orsini, W. E. Geiger, *J. Electroanal. Chem.* **1995**, *380*, 83.

[12] These rhodium fragments also could not be identified after preparative scale electrolysis performed at −2.3 V in the absence of added COD ligand. The indenyl anion was actually formed in quantitative yield but the electron consumption was only one Faraday per mole. This result is surprising since a bielectronic process is expected for the long timescale of electrolysis based on the voltammetric investigation (compare Figure 2). Such a stoichiometry establishes the involvement of a subsequent reaction(s) that is (are) too slow to be observed using voltammetry but sufficiently fast to be active in preparative scale electrolysis. The decrease in the electron consumption, together with the stoichiometric production of indenyl anion, suggests oligomerization of the [Rh(cod)] radical to form cluster compounds under the conditions (concentration) of electrolysis.

[13] A disproportionation such as that shown in equation (7) is a bimolecular process, involving a necessary dependence of the kinetics on the substrate concentration. This is in contrast with the first-order or pseudo-first-order (concentration-independent) kinetics observed here.

[14] Since the electron transfer parameters controlling the second wave were not critical for our simulations, the same value was also used for the second wave, and E_2^0 was then adjusted so that the simulated peak potential values of the second wave reproduced the experimental ones within the range of potential scan rates of interest.

[15] We checked that the introduction of $k_b = 5\,M^{-1}s^{-1}$ did not change the current function of the first peak within the experimental accuracy of its measurement, which accorded with our hypothesis described above.

[16] A more rigorous formulation should consider the fact that the cleavage is an equilibrium. However, as already mentioned, the role of the reverse reaction on the current peak function of the first wave is negligible. This is even more true in the presence of added COD since the reduction becomes more chemically irreversible.

[17] As expected for such a reciprocal formulation, the two points corresponding to the highest values of [COD] appear to be located far away from the line: this is due to the fact that when [COD] is high, the ratio k^*/k_{app} becomes close to unity and a small error in the determination of k_{app} then leads to a huge error in the term on $F(k_{app}) = (k_{app} - k_f)/(k^* - k_{app})$. Nevertheless, the good fit for all other points allowed measurement of the slope.

[18] See, for example: S. Lee, S. R. Lovelace, N. J. Cooper, *Organometallics*, **1995**, *14*, 1974; these authors found a 250 mV separation (in THF) for the two consecutive reduction waves of $[(In)Mn(CO)_3]$ and also invoke a η^5 to η^3 shift. In the case of this indenyl manganese compound, the two reduction waves are chemically reversible, which allows measurement of the two standard potentials E_1^0 and E_2^0, whereas in our case, the second wave is chemically irreversible and controlled by slow charge-transfer kinetics. Thus, E_2^0 cannot be obtained, which prevents a definitive conclusion (as could be drawn in the quoted work on $[(In)Mn(CO)_3]$). Yet, owing to formal identity of the two systems (except for fast subsequent kinetics in our case) it is anticipated that the small value of $(E_1^0 - E_2^0)$ also reflects a change of hapticity.

[19] Here, and in the following, we consider that 17-electron configurations involve changes of hapticity of the indenyl ligand. A partial decoordination of the COD ligand leading to $[(\eta^5\text{-indenyl})(\eta^2\text{-cod})Rh]$ could a priori also be considered. This would be analogous to the structure proposed for the radical anion $[CpCo(cod)]^-$ involving a η^2-cod ligand, ref. [3]. However, this appears rather unlikely in the case of [(In)Rh(cod)] since the indenyl undergoes a very easy η^5 to η^3 slippage compared with Cp (ref. [5]). Additional arguments in favor of a partial decoordination of the indenyl rather than COD can be found 1) in the fact that the indenyl is cleaved, whereas the COD remains coordinated to the metal center and 2) in the easy and fast incorporation of an additional COD ligand; owing to the chelating effect of the COD moiety, replacement of one η^4-cod by two η^2-cod seems highly unlikely.

[20] a) D. J. Kuchynka, J. K. Kochi, *Organometallics*, **1989**, *8*, 677; b) J. Ruiz, M. Lacoste, D. Astruc, *J. Am. Chem. Soc.* **1990**, *112*, 5471.

[21] The new peak potential is more positive than the one observed in the absence of COD. Since the second wave is kinetically controlled by the rate of electron transfer, its peak potential ought to be independent of variations of any follow-up chemical reactions [8]. This means that the potential shift observed in the presence of COD for the second wave arises from a thermodynamic or a kinetic change of the actual electron transfer step. In both cases, this implies a profound structural change of the reduced species vis à vis the case in the absence of COD. This is compatible with the Michaelis–Menten-like formulation in Equations (12) and (13).

[22] H. Estiagh-Hosseini, J. F. Nixon, *J. Less-Common Met.* **1978**, *107*, 61.

[23] M. A. Garralda, L. A. Oro, *Transition Met. Chem.* **1980**, *5*, 65.

[24] C. Amatore, C. Lefrou, F. Pflüger, *J. Electroanal. Chem.* **1989**, *43*, 270.

[25] D. K. Gosser, F. Zhang, *Talanta* **1991**, *38*, 715.